

Redundancy Resolution in Human-Robot Co-Manipulation with Cartesian Impedance Control

F. Ficuciello, L. Villani, and B. Siciliano *

Dipartimento di Ingegneria Elettrica e Tecnologie dell'Informazione,
Università degli Studi di Napoli Federico II, Napoli, Italy
{fanny.ficuciello, luigi.villani, bruno.siciliano}@unina.it

Abstract. In this paper the role of redundancy in Cartesian impedance control of a robotic arm for the execution of tasks in co-manipulation with humans is considered. In particular, the problem of stability is experimentally investigated. When a human operator guides the robot through direct physical interaction, it is desirable to have a compliant behaviour at the end effector according to a decoupled impedance dynamics. In order to achieve a desired impedance behaviour, the robot's dynamics has to be suitably reshaped by the controller. Moreover, the stability of the coupled human-robot system should be guaranteed for any value of the impedance parameters within a prescribed region. If the robot is kinematically or functionally redundant, also the redundant degrees of freedom can be used to modify the robot dynamics. Through an extensive experimental study on a 7-DOF KUKA LWR4 arm, we compare two different strategies to solve redundancy and we show that, when redundancy is exploited to ensure a decoupled apparent inertia at the end effector, the stability region in the parameter space becomes larger. Thus, better performance can be achieved by using, e.g., variable impedance control laws tuned to human intentions.

Keywords: Impedance Control, Redundancy Resolution, Human-Robot Interaction

1 Introduction

In all those applications where robots are used to cooperatively perform operations with humans, intentional human-robot physical interaction is required. Therefore, the stability of the interaction plays an essential role to ensure both safety and high performance. On the other hand, the performance level is related not only to the accuracy of the task execution but also to the comfort perceived by humans during manual guidance. Thus, the ability of the robot to adapt its

* This research has been partially funded by the EC Seventh Framework Programme within the SAPHARI project 287513 and RoDyMan project 320992.

dynamic behaviour to human intentions plays a crucial role. In the robotics literature, different impedance control strategies with modulation of the impedance parameters have been proposed [1–3].

In the application considered here, the robot must be free to move under the forces applied by the operator to the end effector for the execution of a cooperative writing task under human guidance. Hence, a Cartesian impedance strategy is used, where the desired stiffness and the desired position are set to zero while the damping and mass parameters can be suitably tuned. In a recent study [4], we have shown that, for the execution of this kind of co-manipulation task, the performance improves when the robot redundancy is suitably exploited. In detail, the Dynamic Conditioning Index (DCI) presented in [5] has been adopted to solve the redundancy of a 7-DOF KUKA LWR4 arm, with the aim of ensuring a decoupled apparent inertia at the end effector.

In this work, an extensive experimental study is presented, where the role of the redundancy on the stability of the coupled human-robot system is further investigated. In fact, during the interaction, stability depends not only on the implemented control strategy, but also on the robot’s hardware (transmissions, sensors and actuators [6]). Moreover, the more far the desired impedance behaviour is from the natural robot dynamics, the more critical the stability tends to be, and the required control effort becomes more demanding. A theoretical stability analysis provides results that are often too conservative, especially in the presence of redundant degrees of freedom.

By using an experimental procedure, we first find the region in the parameter space (mass and damping) where stability is preserved, taking into account the non-isotropic features of the robot dynamics. Then, the performance of the Cartesian impedance control for different values of the parameters set within the stability region, by using different redundancy resolution strategies, are compared. In particular, the solution based on DCI is confronted to the classical solution based on the maximisation of the kinematic manipulability index. The results show that, using the first solution, the task can be completed for any choice of the impedance parameters (constant or variable) within the stability region. On the other hand, when the manipulability index is adopted, the performance is lower and, in some cases, for parameter values that are close to the frontier but inside the stability region, the task cannot be completed because instability occurs.

2 Impedance control with redundancy resolution

The operator interacts with the robot by grasping the end effector and moving it along arbitrary trajectories. It is assumed that only forces can be applied. Since the robot’s tip has to follow and adapt to the applied force, the end-effector dynamics can be set as a mass-damper system of equation

$$\mathbf{A}_d \ddot{\mathbf{x}} + \mathbf{D}_d \dot{\mathbf{x}} = \mathbf{F}_{ext}, \quad (1)$$

where $\mathbf{x} \in \mathbb{R}^3$ is the Cartesian position vector of the robot's tip, $\mathbf{F}_{ext} \in \mathbb{R}^3$ is the vector of the external forces and \mathbf{A}_d and \mathbf{D}_d are suitable inertia and damping matrices, that here are set as constant diagonal matrices.

The control law that imposes the impedance dynamics (1) can be implemented in the joint space in the form:

$$\boldsymbol{\tau}_{imp} = -\mathbf{J}^T(\mathbf{q})\mathbf{A}(\mathbf{q})[\dot{\mathbf{J}}\dot{\mathbf{q}} + \mathbf{A}_d^{-1}(\mathbf{D}_d\dot{\mathbf{x}} - \widehat{\mathbf{F}}_{ext})] + \mathbf{g}(\mathbf{q}) - \mathbf{r}, \quad (2)$$

where $\mathbf{q} \in \mathbb{R}^n$, with $n = 7$, is the vector of joint variables, $\mathbf{J}(\mathbf{q})$ is the robot Jacobian mapping $\dot{\mathbf{q}}$ to $\dot{\mathbf{x}}$ and $\mathbf{A}(\mathbf{q})$ is a (3×3) positive definite inertia matrix in the operational space [7].

In the above control law, an estimation of the external force $\widehat{\mathbf{F}}_{ext}$ is employed, assuming that force sensors on the end effector are not available. The estimation is computed using the residual technique developed in [8], as $\widehat{\mathbf{F}}_{ext} = \mathbf{J}^{\dagger T}(\mathbf{q})\mathbf{r}$, where the dynamically consistent generalised inverse of the Jacobian

$$\mathbf{J}^{\dagger}(\mathbf{q}) = \mathbf{M}^{-1}(\mathbf{q})\mathbf{J}^T(\mathbf{q})[\mathbf{J}(\mathbf{q})\mathbf{M}^{-1}(\mathbf{q})\mathbf{J}(\mathbf{q})^T]^{-1}$$

is used, being $\mathbf{M}(\mathbf{q})$ the positive definite inertia matrix of the robot in the joint space. Vector \mathbf{r} is the residual providing an estimate of the external torques acting on the robot, that can be computed on the basis of the robot dynamic model and on the control torques.

In the application considered here, the human guidance of the end effector involves 3 of the 7 degrees of freedom of the KUKA LWR4 robot, thus there are 4 redundant degrees of freedom at disposal for a secondary task in the null space of the end-effector task. Our aim is to use these additional degrees of freedom to improve the effectiveness of the end-effector task, in terms of stability and performance.

The control law with redundancy resolution is:

$$\boldsymbol{\tau}_c = \boldsymbol{\tau}_{imp} + (\mathbf{I} - \mathbf{J}^T\mathbf{J}^{\dagger T})(\mathbf{u} - k_D\dot{\mathbf{q}}), \quad (3)$$

where $-k_D\dot{\mathbf{q}}$, with $k_D > 0$, is a suitable damping torque and \mathbf{u} is a torque vector to be designed, corresponding to a secondary task, that can be set as:

$$\mathbf{u} = k_c \left(\frac{\partial \omega(\mathbf{q})}{\partial \mathbf{q}} \right)^T, \quad (4)$$

being $k_c > 0 (< 0)$ if the performance index has to be maximised (minimised).

2.1 Performance indices

Different criteria can be pursued in order to choose the performance index corresponding to the secondary task.

One common choice is the kinematic manipulability index, proportional to the area of the velocity manipulability ellipsoid, which represents the capability of the robot to move the end effector along the Cartesian directions, with a

given set of unit norm joints velocities. Hence, in a joint configuration where this index is (locally) maximised, it is possible to produce end-effector velocities in all possible directions with (locally) minimal joint velocities. The manipulability index (see, e.g., [9]) is defined as:

$$m(\mathbf{q}) = \sqrt{\det(\mathbf{J}\mathbf{J}^T)}, \quad (5)$$

i.e., by choosing \mathbf{u} in (3) as

$$\mathbf{u} = k_m \nabla m(\mathbf{q}),$$

where the gradient of the manipulability measure $\nabla m(\mathbf{q})$ can be computed as [10]:

$$\nabla m(\mathbf{q}) = \frac{\partial m(\mathbf{q})}{\partial q_i} = m(\mathbf{q}) \text{trace} \left[\frac{\partial \mathbf{J}}{\partial q_i} \mathbf{J}^\dagger \right]. \quad (6)$$

Another possibility of exploiting redundancy is that of trying to optimise in some way the mapping between the forces applied to the end effector and the corresponding velocities or accelerations. As a matter of fact, in ideal conditions, the Cartesian impedance control law (2) allows cancelling out the robot dynamics as well as making the end-effector dynamics completely independent of the joint configuration. The most critical element is the equivalent inertia $\mathbf{A}(\mathbf{q})$, which is coupled and configuration dependent. At any given end-effector position, what can be done is to exploit the internal motion to move the robot towards configurations with maximally decoupled inertia. This can be achieved as in [4], by using a task function inspired to the dynamic conditioning index (DCI) introduced by [5] to measure the dynamic isotropy of robot manipulators in joint space.

In the operational space, the DCI index can be defined as the least-square difference between the generalized inertia matrix and an isotropic matrix, as:

$$\omega(\mathbf{q}) = -\frac{1}{2} \mathbf{E}(\mathbf{q})^T \mathbf{W} \mathbf{E}(\mathbf{q}) \quad (7)$$

where \mathbf{W} is a diagonal weighting matrix and the error vector $\mathbf{E}(\mathbf{q})$ is defined as $\mathbf{E}(\mathbf{q}) = [\lambda_{11}(\mathbf{q}) - \sigma(\mathbf{q}), \lambda_{22}(\mathbf{q}) - \sigma(\mathbf{q}), \lambda_{33}(\mathbf{q}) - \sigma(\mathbf{q}), \lambda_{12}(\mathbf{q}), \lambda_{13}(\mathbf{q}), \lambda_{23}(\mathbf{q})]^T$, with σ defined as

$$\sigma(\mathbf{q}) = \frac{1}{3} \text{Tr}(\mathbf{A}(\mathbf{q})).$$

The weighting matrix \mathbf{W} has been chosen in order to give priority to the minimization of the norm of the off-diagonal elements of $\mathbf{A}(\mathbf{q})$, as $\mathbf{W} = \text{diag}\{\mathbf{I}_3, 5\mathbf{I}_3\}$.

3 Variable damping

A variable damping strategy has been selected to vary the damping properties of the end effector in order to accommodate the human movement during physical interaction. According to the results available in literature [3, 6, 1], the human perception is mainly influenced by the damping parameter, while, for a

given damping, the desired mass determines the bandwidth of the system, and the stability. High damping values are desired when the operator performs fine movements while lower values should be used for fast movements.

In the next Section, the stability region in the parameter space will be evaluated experimentally for any damping value in the interval $[5, 60]$ Ns/m. The damping must be decreased if the operator wants to accelerate and increased if (s)he wants to decelerate and the desired mass have to be chosen accordingly.

In order to generate a law for the variable damping that is smooth also for sudden changes of the direction of motion, the damping can be related to the absolute value of the velocity.

When the operator wants to accelerate (decelerate) in a certain direction of the Cartesian space the velocity increases (decreases); thus, by decreasing (increasing) the damping accordingly, the impedance control strategy will accommodate the intention of the operator. The relationships used to vary the damping for each of the Cartesian principal directions is

$$D = a e^{-b|\dot{x}|}. \quad (8)$$

whit $a = 60$ and $b = 4$. These parameters have been chosen empirically in order to have a variation of the damping within the interval $[5, 60]$ Ns/m for the possible range of velocities in the considered task.



Fig. 1. Starting configuration for the writing task.

4 Experimental Results

In this Section, the two performance indices for redundancy resolution presented in Section 2 are evaluated and compared experimentally in terms of stability and performance.

A case study has been selected, consisting in the execution of a writing task on a horizontal plane operated by a human: the operator guides a paint marker mounted on the robot's tip along a path drawn on a paper sheet. The initial configuration of the robot, shown in Fig. 1, has been chosen to facilitate the execution of the task. A snapshot of the task execution is reported in Fig. 2.

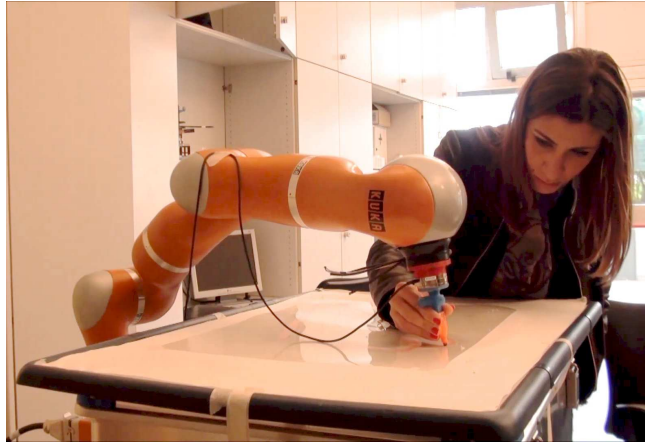


Fig. 2. Snapshot of the co-manipulation task.

4.1 Stability

In our previous paper [4] the allowed range of variation of the impedance parameters of (1), so that stability is preserved, was evaluated experimentally. The corresponding stability region in the parameter space was found by setting the same damping and mass parameters along all the Cartesian directions. This choice was rather conservative, considering that, e.g., the equivalent inertia at the end effector in the configuration of Fig. 1 is non homogenous being the inertia moment about the vertical direction almost ten times higher than the inertia moments about the horizontal axes. In this work, by using the same experimental procedure described in [4], a more accurate evaluation of the stability region has been carried out, but allowing the choice of different values of the parameters along the three Cartesian directions. The stability regions for the three Cartesian directions of the end effector, referred to the base frame, are shown in Fig. 3. The parameters are the desired damping D along a given Cartesian

direction and the desired time constant T of the impedance equation (1), defined as D/λ , being λ the desired mass along the same Cartesian direction.

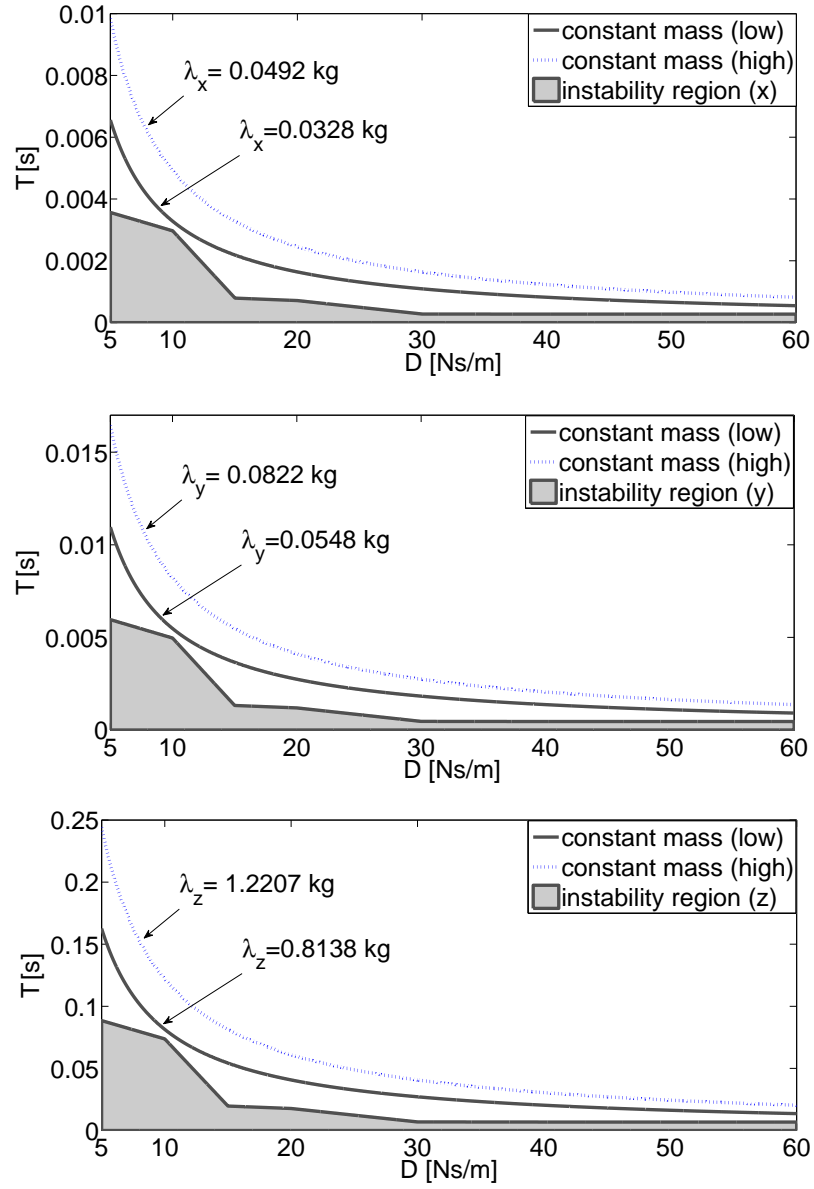


Fig. 3. Stability regions and constant mass curves for the three Cartesian directions.

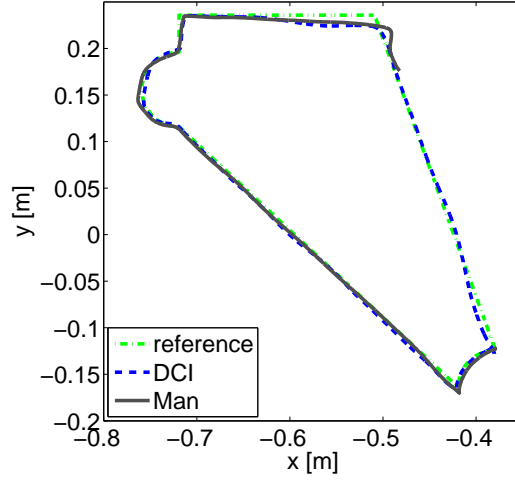


Fig. 4. Reference and actual paths for the writing task in the case of low desired inertia.

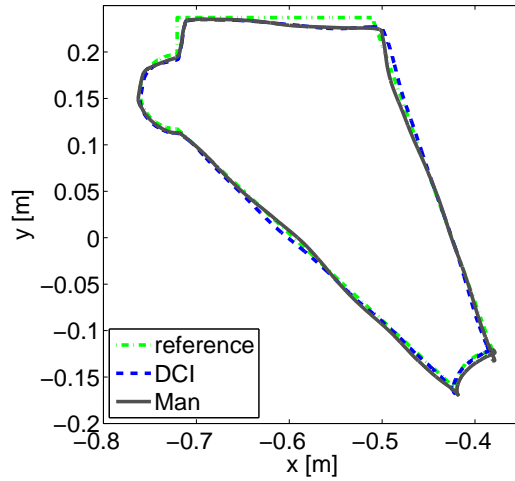


Fig. 5. Reference and actual paths for the writing task in the case of high desired inertia.

In the same figure, two set of curves corresponding to two different values of the mass for each Cartesian direction are represented. The curves with $\mathbf{A}_d = \text{diag}\{0.0328, 0.0548, 0.8138\}$ kg constant mass are close to the instability frontiers, and can be assumed as minimal inertia curves. The dashed curves, with $\mathbf{A}_d = \text{diag}\{0.0492, 0.0822, 1.2207\}$ kg, are safely within the stability regions.

In the first set of experiments, the comparison between the two redundancy resolution strategies is carried out by checking the stability, i.e., by verifying

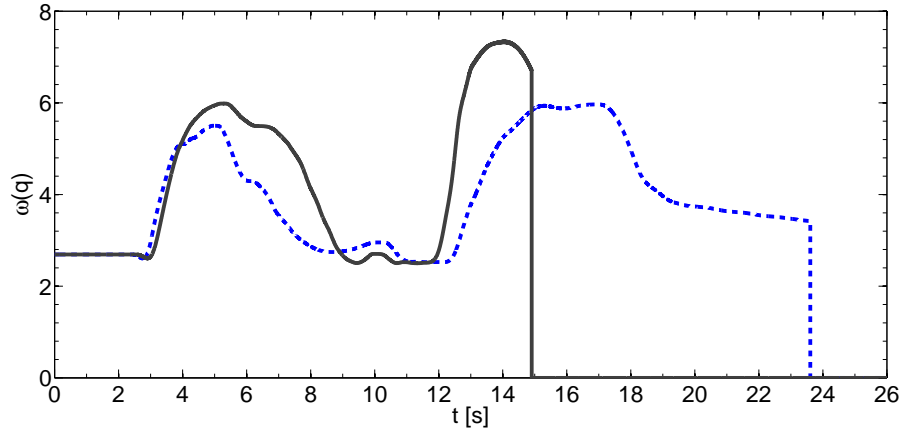


Fig. 6. Time histories of the values of DC index in the case of low desired inertia and variable damping. The continuous (dashed) line represents the index when redundancy is used to increase manipulability (to minimise the DC index).

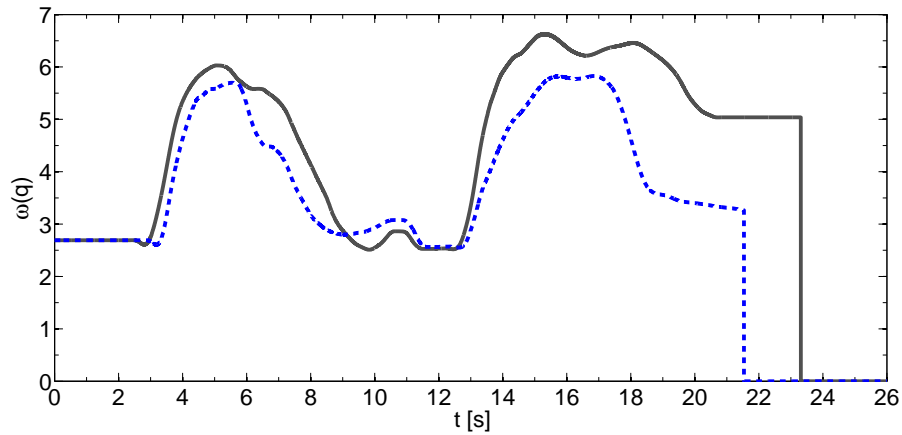


Fig. 7. Time histories of the values of DC index in the case of high desired inertia and variable damping. The continuous (dashed) line represents the index when redundancy is used to increase manipulability (to minimise the DC index).

experimentally that the system remains stable during the task execution. The comparison have been performed for both constant and variable damping. The variable damping has been set according to Eq. (8) while the masses have been set constant, so that the impedance parameters vary on the constant mass curves of Fig. 3.

When the DC index is used for redundancy resolution, the task has been completed in both cases corresponding to low and high values of desired inertia,

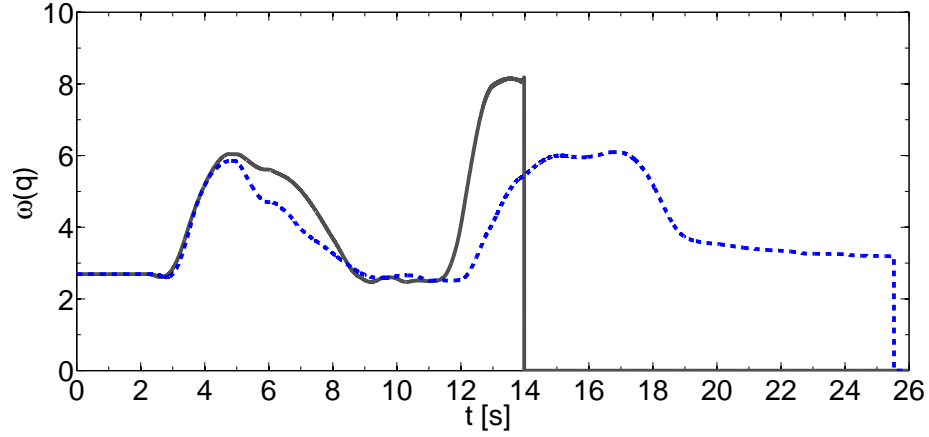


Fig. 8. Time histories of the values of DC index in the case of low desired inertia and constant damping.. The continuous (dashed) line represents the index when redundancy is used to increase manipulability (to minimize the DC index).

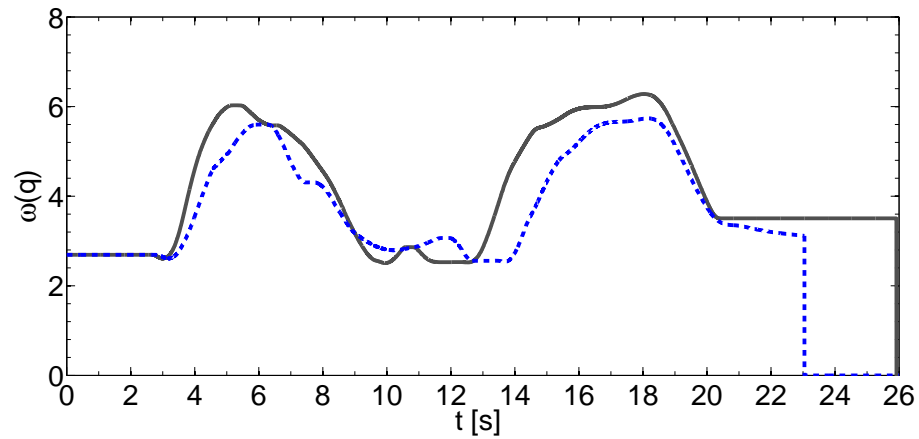


Fig. 9. Time histories of the values of DC index in the case of high desired inertia and constant damping. The continuous (dashed) line represents the index when redundancy is used to increase manipulability (to minimize the DC index).

as it is shown in Figs. 4 and 5, where the paths of the paint marker are represented together with the reference path.

On the other hand, in the case of low inertia (Fig. 4), the task cannot be completed when the manipulability (Man) index is used for redundancy resolution, because the system tends to become unstable.

The corresponding time histories of the DC index during the execution of the experiment are reported in Figs. 6 and 7 respectively.

Notice that the values of the DC index are always lower when the minimization of the DC index is used as secondary task, as expected, with some exceptions in correspondence of abrupt changes of directions. Moreover, in the case of low inertia, the system tends to become unstable when the value of the DC index is too high, i.e., when the inertia of the robot at the end effector deviates significantly from the desired diagonal inertia imposed by the control.

Similar results can be observed in the case that the damping has been set constant (to the value of 60 Ns/m). The corresponding time histories of the DC index are reported in Figs. 8 and 9.

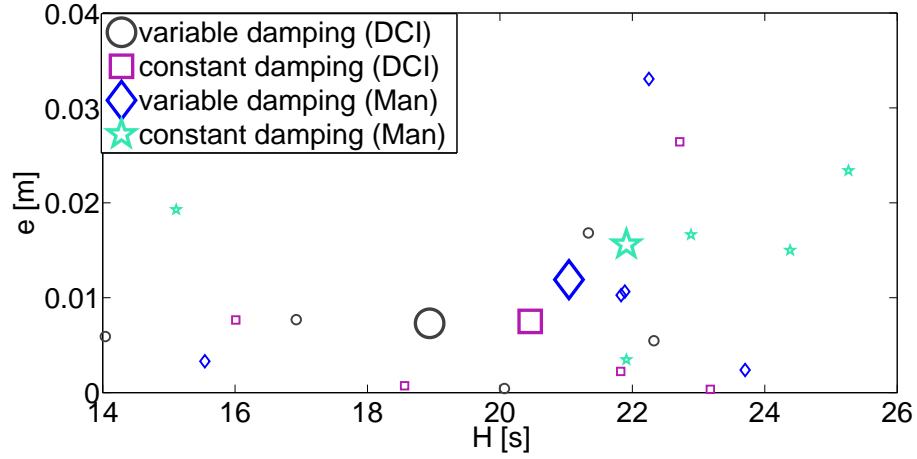


Fig. 10. Values of the length error e and execution time H in the experiments on five subjects using variable and constant impedance; both manipulability and DC index optimisation are used as secondary tasks. The bigger markers are the mean values on the five different subjects.

4.2 Performance

The second set of experiments is aimed at evaluating the performance related to the two redundancy resolution strategies in terms of accuracy and execution time of the writing task. The accuracy has been measured by considering the error between the length of the path drawn in cooperation with the robot, l_e , and the ideal path length, l_d , namely:

$$e = |l_d - l_e|. \quad (9)$$

The execution time H is defined as the difference between the time when the entire path is completed and the time when the drawing tool touches the paper on the desk to start writing.

Two different impedance laws have been considered, one with constant parameters (set as $\lambda = 1.1$ kg, $D = 60$ Ns/m) and the other with variable damping (according to Eq. (8)) and constant mass (set as $\lambda = 1.1$ kg.). For simplicity, the impedance parameters have been set equal in all the Cartesian directions. The tests have been carried out on five different subjects that move the robot using their dominant hand. Each subject has been trained in advance, by executing the task with the different strategies to be tested. During the training phase, each subject was asked to look for the configuration which resulted the most comfortable, as well as for the best fitting starting point of the path, without any kind of conditioning. Moreover, they have been requested to pursue accuracy as a primary objective and execution time as a secondary objective. In addition, both during the training phase and the actual testing phase, the subjects have not been informed on the features of each control law, nor even which one of the four algorithms they were testing.

The results of the tests carried out both with constant and variable impedance are shown in Fig. 10, where the error on the length of the path e versus the execution time H is reported for all the subjects, as well as their mean values. In our previous work [4] the experimental results have shown that the error on the path is substantially reduced when a secondary task (exploiting DCI) is imposed. The experiments presented here confirm that the use of the DC index ensures better performance also with respect to other kind of secondary tasks, as that based on the kinematic manipulability index. Notice that, in the variable damping case, a significant reduction of the error on the path is obtained in spite of the strategy used to solve the redundancy.

Last but not least, all the subjects involved in the experiments have verified that the “feeling” of the manual guidance (in terms of intuitiveness and response of the robot) improves when the DC index is adopted, i.e., when redundancy is used to decouple the natural end-effector dynamics along the principal directions of the task and a further improvement is experienced when the damping parameters are tuned online according to the law (8).

5 Conclusions

A Cartesian impedance strategy with redundancy resolution has been proposed to control a 7-DOF KUKA LWR4 arm for a human-robot co-manipulation task. Experimental tests have shown the importance of exploiting the redundancy for both stability and performance. Two different strategies to solve redundancy, one based on the dynamic conditioning index and the other based on the kinematic manipulability index, have been compared and the corresponding stability regions have been found. The experiments have evidenced that, if redundancy is designed to minimise the coupling of the end-effector equivalent inertia, the stability region in the impedance parameters space is enlarged. Moreover, the use of the dynamic conditioning index allows to improve accuracy and execution time both for constant and variable impedance control.

References

1. R. Ikeura, T. Moriguchi, and K. Mizutani, "Optimal variable impedance control for a robot and its application to lifting an object with a human," in *IEEE Int. Workshop on Robot and Human Interactive Communication*, Berlin, Germany, 2002, pp. 500–505.
2. T. Tsumugiwa, R. Yokogawa, and K. Hara, "Variable impedance control based on estimation of human arm stiffness for human-robot cooperative calligraphic task," in *IEEE Int. Conf. on Robotics and Automation*, Washington, DC, USA, 2002, pp. 644–650.
3. A. Lecours, B. Mayer-St-Onge, , and C. Gosselin, "Variable admittance control of a four-degree-of-freedom intelligent assist device," in *IEEE Int. Conf. on Robotics and Automation*, Saint Paul, Minnesota, USA, 2012, pp. 3903–3908.
4. F. Ficuciello, A. Romano, L. Villani, and B. Siciliano, "Cartesian impedance control of redundant manipulators for human-robot co-manipulation," in *IEEE/RSJ Int. Conf. on Intelligent Robots and Systems*, Chicago, USA, 2014, p. to appear.
5. O. Ma and J. Angeles, "The concept of dynamic isotropy and its applications to inverse kinematics and trajectory planning," in *IEEE Int. Conf. on Robotics and Automation*, San Francisco, CA, 1990, pp. 10–15.
6. V. Duchaine, B. Mayer-St-Onge, D. Gao, and C. Gosselin, "Stable and intuitive control of an intelligent assist device," *IEEE Transactions on Haptics*, vol. 5, no. 2, pp. 1939–1412, 2012.
7. O. Khatib, "A unified approach for motion and force control of robot manipulators: The operational space formulation," *IEEE Journal of Robotics and Automation*, vol. 3, no. 1, pp. 1115–1120, 1987.
8. A. D. Luca, A. Albu-Schäffer, S. Haddadin, and G. Hirzinger, "Collision detection and safe reaction with the DLR-III lightweight robot arm," in *IEEE/RSJ Int. Conf. on Intelligent Robots and Systems*, Beijing, China, 2006, pp. 1623–1630.
9. H. Sadeghian, F. Ficuciello, L. Villani, and M. Keshmiri, "Global impedance control of dual-arm manipulation for safe human-robot interaction," in *10th IFAC Symposium on Robot Control*, Dubrovnik, Croatia, 2012, pp. 767–773.
10. J. Park, W. Chung, and Y. Youm, "Computation of gradient of manipulability for kinematically redundant manipulators including dual manipulators system," *Transaction on Control Automation, and Systems Engineering*, vol. 1, no. 1, pp. 8–15, 1999.